water

MDPI

Article

Permanganate/Bisulfite Pre-Oxidation of Natural Organic Matter Enhances Nitrogenous Disinfection By-Products Formation during Subsequent Chlorination

Shu He [1,2] and Nanqi Ren [1,3,*]

[1] School of Environment, Harbin Institute of Technology, Harbin 150090, China; heshu@yctesting.com
[2] Shenzhen Yuchi Testing Technology Co., Ltd., Shenzhen 518055, China
[3] State Key Laboratory of Urban Water Resource and Environment, School of Civil and Environmental Engineering, Harbin Institute of Technology (Shenzhen), Shenzhen 518055, China
* Correspondence: rnq@hit.edu.cn

Abstract: The permanganate/bisulfite (PM/BS) process is a novel oxidation process, which can degrade micropollutants within several seconds. As natural organic matter (NOM) ubiquitously exists in an aquatic environment, the PM/BS process will inevitably react with NOM, which may impact the disinfection-by-products (DBPs) formation during subsequent chlorination. This study investigated the effect of PM/BS pre-oxidation of NOM on DBP formation. It was found that TOC removal reached a plateau when the molar ratio of PM to BS was 1:5. Increasing ratios of PM to BS decreased the intensity and area of fluorescence spectroscopy. PM and BS doses, pre-oxidation time, pH of solutions and concentration of Br^- impacted the formation potential of various DBPs. PM/BS pre-oxidation decreased the formation of TCM while increasing the yields of N-DBPs, thus increasing the risk of water quality. Calculated toxicity analysis showed that a general increase in CTI was observed with PM/BS pre-oxidation, indicating that PM/BS pre-oxidation had a negative effect on risk control of overall cytotoxicity. Although the PM/BS process could accelerate the degradation of micropollutants, the elevated DBPs formation, especially highly toxic N-DBPs, needs enough attention to control water-quality risk.

Keywords: natural organic matter; permanganate/bisulfite; disinfection by-products; chlorination

Citation: He, S.; Ren, N. Permanganate/Bisulfite Pre-Oxidation of Natural Organic Matter Enhances Nitrogenous Disinfection By-Products Formation during Subsequent Chlorination. *Water* **2022**, *14*, 507. https://doi.org/10.3390/w14030507

Academic Editor: Huiyu Dong

Received: 28 November 2021
Accepted: 26 January 2022
Published: 8 February 2022

1. Introduction

Drinking-water disinfection is an indispensable treatment process to protect humans from epidemic disease. Among the various disinfectants, chlorine was extensively employed to improve water quality since the 20th century [1]. However, numerous organic materials in water may react with chlorine to yield unintended disinfection by-products, such as trihalomethanes (THMs) and haloacetic acids (HAAs). Public concern about DBPs has prompted the investigation of the possible association between chlorination by-products and human health [2]. Although the characteristics and toxicity of many DBPs remain unclear, several studies have shown that frequent exposure to DBPs may increase the risk of bladder cancer [2,3].

Natural organic matter (NOM), a complex heterogeneous mixture composed of humic acid (HA), fulvic acid (FA) and humin, is considered to be the precursor of DBPs [4,5]. Several techniques, including ultraviolet/visible (UV-vis) spectroscopy, Fourier transform infrared (FT-IR) spectroscopy and three-dimensional fluorescence excitation–emission matrix (3D-EEM) spectroscopy, have been applied to obtain the characteristics of NOM. The measurement of UV-visible spectroscopy is a fast and cheap method with no specific sample preparation to provide the information about chromophores in NOM [6]. Roccaro et al. found the correlations between the differential absorbance at 272 nm and the formation potential of DBPs in different parameters [7]. The 3D-EEM spectroscopy technique has

recently gained popularity to characterize fluorophores of organic matter according to the fluorescence intensity and peak maxima. The structure, fate and reactivity of dissolved organic matter in a global range of environments are associated with the molecular weight measured by high-pressure size-exclusion chromatography (HPSEC). NOM can be removed through coagulation with aluminum salt and absorption. Due to the increase in turbidity and organic materials in raw water, NOM cannot be effectively removed through traditional water-treatment processes (e.g., coagulation, sedimentation and filtration) [8]. Pre-oxidation, which can decompose complex matter into a compound with smaller molecular weight and easier structure, has been widely implemented to control the concentration of DBPs' precursors [9,10]. The removal of NOM by traditional processes can be improved by an appropriate pre-oxidation process. Among various pre-oxidants, including chlorine, chlorine dioxide, hydrogen peroxide, ozone and potassium permanganate (PM), PM is an environmentally friendly and modest-cost manganese-containing material. However, some refractory organic pollutants cannot be degraded by PM. Moreover, an increased dosage of PM may deepen the color of raw water [11].

In recent years, many kinetic studies of PM have been successively carried out to enhance the oxidizing ability of PM for certain pollutants. Studies by Sun and other investigators have demonstrated that PM can be activated using bisulfite to generate soluble Mn (III) that plays important roles in water treatment [12,13]. They found that the degradation rate of phenol, ciprofloxacin and methyl blue at pH_{ini} 5.0 were 5–6 orders of magnitude faster than those measured for PM alone. As a novel oxidation process, the PM/BS system is used to remove a typical amino acid, which showed that the removal rates of dissolved organic nitrogen and glutamate in PM/BS within 10 min were 55% and 90%, respectively. Subsequent electronic spin resonance (ESR) experiments showed that Mn (III), SO_3^- and ·OH were involved in the degradation process [14]. Gao et al. [15] have reported that the degradation of an emerging endocrine disruptor, bisphenol S (BPS), by the PM/BS system at pH 4 to 7 was 6–7 orders of magnitude faster than those for permanganate alone. Most researchers have ascribed the enhancement of degradation efficiency of target pollutants to the involvement of Mn (III). Several complex ligands, including pyrophosphate, nitrilotriacetate and humic acid, were used to see their effects on the oxidation of triclosan (TCS).

Even though the use of PM/BS is emerging, previous studies have focused on the powerful oxidation towards typical pollutants. Therefore, the main purpose of this study is to analyze the structural changes of NOM through TOC, UV-Vis and 3D-EEM after pre-oxidation by the PM/BS system and evaluate the effects of PM, BS dosage, pre-oxidation time, pH and concentration of Br^- on the formation potential of C-DBPs and N-DBPs. These efforts may render a better understanding on the NOM characterization and benefit the development of a feasible strategy to control chlorination-disinfection by-products.

2. Materials and Methods

2.1. Materials

Unless otherwise noted, all reagents used in this study were of reagent grade, and solutions were prepared with ultrapure water (18.2 MΩ cm) produced by a Milli-Q system (Advantage A10, Millipore, MA, USA). Potassium permanganate, sodium phosphate dibasic dodecahydrate, sodium dihydrogen phosphate dehydrate, potassium dihydrogen phosphate dodecahydrate, ethylenediamine tetraacetic acid disodium salt, sodium bisulfite, sodium hypochlorite, sulfuric acid, sodium hydroxide and anhydrous sodium sulfate were purchased from Sinopharm Chemical Reagent Co., Ltd. (Beijing, China). Methyl tert-butyl ether (MTBE) was purchased from J&K Chemical (Shanghai, China). Humic acid was provided by Sigma-Aldrich (St. Louis, MO, USA).

2.2. Experimental Procedures

2.2.1. Pre-Oxidation

PM/BS pre-oxidation was carried out in a 50 mL conical flask with cover at a controlled room temperature. Amounts of 250 μM of BS and 50 μM of PM were simultaneously added to the aqueous solution containing humic acid (3 mg L^{-1}). HA alone and HA/PM were also set as controls. After the reaction solution was stirred on a magnetic stirrer for 30 min, the samples were then transferred into capped amber glass for later analysis.

2.2.2. Formation Potential of Disinfection By-Products

An amount of 20 mg L^{-1} of NaClO was added to the aqueous solution, and then the concentration of residual chlorine was measured after 5 min of PM and PM/BS systems. According to the differentials between the two systems, an appropriate dose of NaClO was added to the PM/BS system to achieve a final concentration of 20 mg L^{-1} for NaClO. These samples were stored in dark for 24 h. After chlorination, three C-DBPs and three N-DBPs were analyzed by liquid–liquid extraction with MTBE, performing derivatization with acidified methanol and quantification by GC/ECD.

2.3. Analysis

2.3.1. TOC, UV_{254}, UV-Vis and Residual Chlorine

Total organic carbon (TOC) was measured by TOC analyzer (Shimadcu, Japan). The UV-Vis absorbance spectrum of NOM was determined by ultraviolet and visible spectrophotometer (DR 5000, HACH) by scanning from 200 to 800 nm as compared to a blank of Milli-Q water. In this study, N.N-diethyl-p-phenylenediamine spectrophotometric method was used to determine the amount of residual chlorine. To be specific, 0.5 mL of samples were added to a glass bottle, which contained 4.5 mL of water. Then, 750 μL of phosphate buffer at pH 6.5 and 250 μL of DPD solution were introduced to the mixture. UV spectrophotometer (DR 6000, HACH) was used to measure the absorbance at 515 nm. The chlorine concentration can be calculated based on the absorbance and standard curve.

2.3.2. Three-Dimensional-EEM

Fluorescence EEM measurements were conducted in a 1.0 cm quartz cell using a fluorescence spectrofluorometer (Cary eclipse, Agilent) at room temperature. The spectrofluorometer used a xenon excitation source to generate excitation-emission matrices (EEMs) for each sample over excitation wavelengths between 200–400 nm in 5 nm intervals and emission wavelength between 280–550 in 5 nm intervals.

2.3.3. DBPs Analysis

Trichloromethane (TCM), dichloropropanone (DCP), trichloropropanone (TCP), trichloroacetonitrile (TCAN), dichloroacetonitrile (DCAN) and trichloronitromethane (TCNM) were measured by gas chromatography (7890, Agilent, CA, USA) equipped with an electron capture detector (ECD) based on the modified USEPA method 551.1 after samples were extracted with methyl tert-butyl ether [16]. The capillary column used for the analyses was an HP-5 (30 m × 0.25 mm, 0.25 μm, J&W, Folsom, CA, USA). The oven-temperature program was as follows: injector temperature at 200 °C; detector temperature at 300 °C and column temperature at 40 °C (held for 5 min), increased to 45 °C with the rate of 1 °C min^{-1} (held for 3 min), increased to 135 °C with the rate of 10 °C min^{-1} and then increased to 220 °C with the rate of 25 °C min^{-1}. The limits of quantification of C-DBPs and N-DBPs were around 0.1–0.15 ug L^{-1}.

All experiments were replicated at least twice, and the reported data present the average of experimental results.

3. Results and Discussion

3.1. Characterization of NOM

3.1.1. UV-Visible Absorption Spectroscopy of NOM

UV-Vis spectroscopy is a relatively effective method to provide information about the chromophoric group without special pretreatment for the sample [16,17]. The UV-visible absorption spectra in different systems are illustrated in Figure 1a. HA alone had no characteristic absorption peak due to its wide molecular-weight distribution, complicated structure and interactions between functional groups. Although the characteristic absorption peak for PM at 515 nm still existed in the PM system, it completely disappeared when BS was introduced to activate PM. Meanwhile, the absorbance value of PM/BS decreased significantly, which means the chromophoric groups may have oxidized during this process. The UV-visible absorption spectra obtained from different PM and PM/BS doses are shown in Figure 1b,c. With the concentration of PM to BS increased, the absorbance value also increased gradually. Note that the absorption peak at 525 nm for PM did not vanish even when the concentration reached 250 μM, indicating that the oxidation of NOM by PM is a slow reaction.

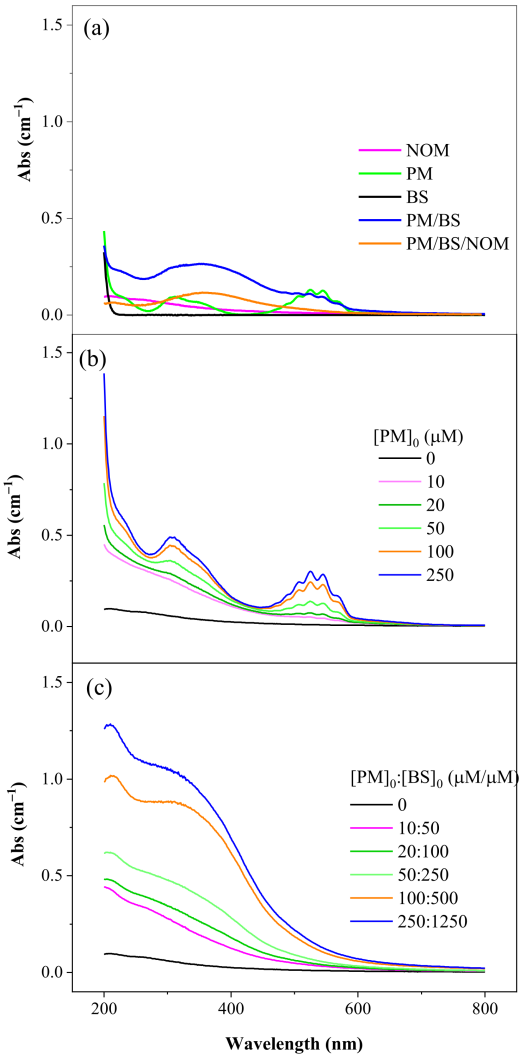

Figure 1. The UV-visible absorption spectra in different oxidation systems (**a**). ($(HA)_o$ = 3 mg L^{-1}, $(PM)_o$ = 50 μM, $(BS)_o$ = 250 μM and t = 30 min). The UV-visible absorption spectra obtained from different PM (**b**) and PM/BS doses (**c**). ($(HA)_o$ = 3 mg L^{-1}, $(PM)_o$ = 0–250 μM, $(BS)_o$ = 0–1250 μM and t = 30 min).

3.1.2. TOC Removal

Figure 2 presents the TOC removal rate in different molar ratios of PM to BS. The molar ratio of the PM/BS was increased from 1:1 to 1:10 while the initial concentration of TOC was kept at 3 mg L^{-1}. The TOC removal rate was 2% when the dosage of PM alone was 50 μM. After the introduction of BS, the removal rate continuously increased as the PM/BS molar ratios increased from 1:1 to 1:5 but decreased significantly when the ratio was 1:10. This trend was similar to the investigation that explored the effects of molar ratios of PM/BS to the degradation efficiency of BPS conducted by Gao et.al (2017). Results showed that the degradation of BPS reached a maximum as the ratio was 1:10 and rapidly dropped when the ratio was continuously increased. This can be explained by noting that, in the case of excessive BS, trivalent manganese will be consumed by HSO_3^-, resulting in the declination of the TOC removal rate. Meanwhile, the TOC removal rates under various PM and PM/BS dosages are also investigated. As demonstrated in Figure S1 (Supplementary Materials), the TOC removal rate increased with the increase in PM/BS doses.

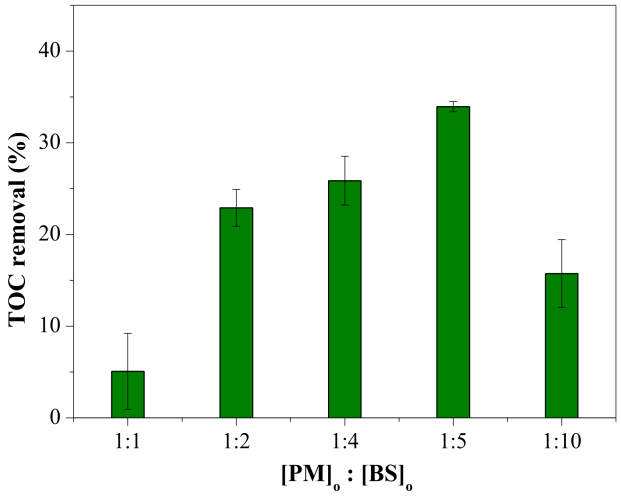

Figure 2. Removal of TOC by PM/BS process with different molar ratios of PM to BS. ($(HA)_o$ = 3 mg L^{-1}, t = 30 min and $(PM)_o$:$(BS)_o$ = 1:1–1:10). Duplicated samples were analyzed.

3.1.3. Three-Dimensional Fluorescence Excitation–Emission Matrices of NOM

The fluorescence excitation–emission matrices for HA alone, PM pre-oxidation and PM/BS pre-oxidation are illustrated in Figure S2 (Supplementary Materials). Generally, the fluorescence spectrum could be roughly divided into five regions according to the position of the fluorescence peak, representing five different categories of NOM. The positions of region I and region II were in Ex/Em = 200–250 nm/280–320 nm and Ex/Em = 200–250 nm/320–380 nm, respectively, which mainly represented aromatic proteins. The position of region III in Ex/Em = 200–250 nm/380–500 nm represents the fulvic acid. Zone IV was located at Ex/Em = 250–280 nm/280–380 nm, representing soluble microbial products (SMPs), and zone V was located at Ex/Em = 250–400 nm/380–500 nm, representing humic acids. The peak locations of HA alone, which were in accordance with previous results, indicated the existence of fulvic-like components [18]. After pre-oxidation with PM, the intensity of the fluorescence peak in region III decreased from 95.8 to 89.3 and eventually vanished in the PM/BS system, which indicated the destruction of the chromophoric group. Figure 3 demonstrates the fluorescence excitation-emission matrices obtained from different ratios of PM to BS. The removal of NOM sharply increased with the PM to BS ratios changing from 10:50 μM up to 100:500 μM. The EEM spectrum exhibited similar trends under a different molar ratio of PM to BS (Figure S3, Supplementary Materials). A study claimed that the fluorescence peaks for raw water samples decreased after exposure to ozone. The addition of pre-ozonation also reduced the intensity of microbial protein-like substances and marine humic-like compounds, which

was similar to our investigations [19]. It is noteworthy that the position of two peaks on the EEM spectra shifted along the direction of increasing wavelength after treatment with BAC filter. These results reflect that the increase in functional groups was different from our own results, which showed no significant change.

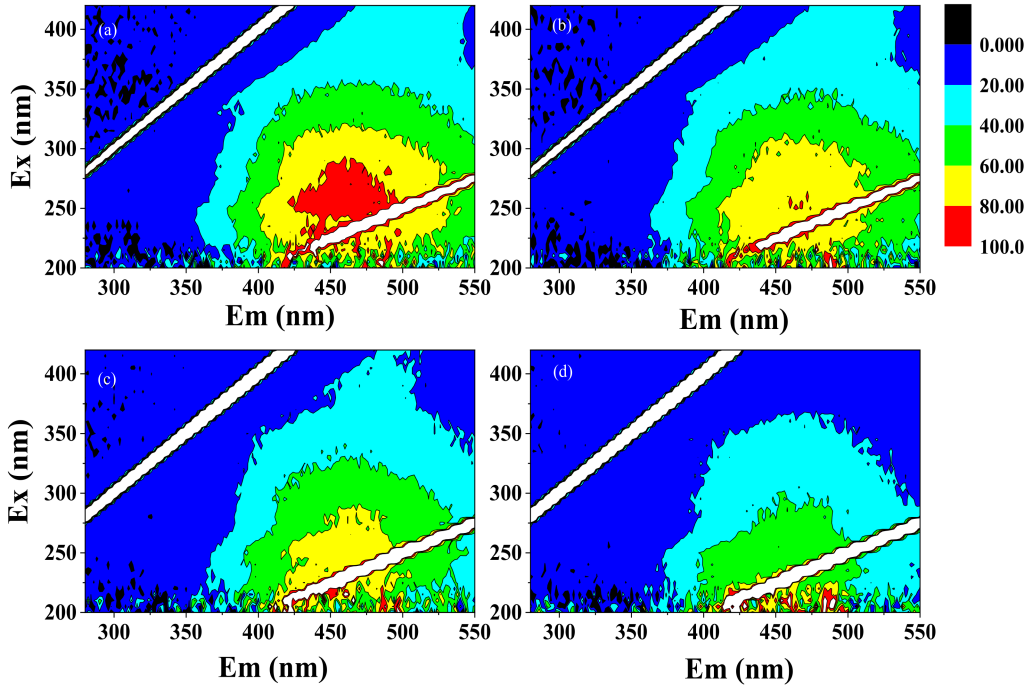

Figure 3. The fluorescence excitation-emission matrices obtained from different ratios of PM to BS. (**a**) 10:50 μM:μM, (**b**) 20:100 μM:μM, (**c**) 50:250μM:μM and (**d**) 100:500 μM:μM. ((HA)o = 3 mg L^{-1} and (PM)o:(BS)o = 10:50–100:500 μM:μM).

3.2. Formation Potential of DBPs from NOM

3.2.1. Effects of PM and BS Doses

In this study, six by-products were identified and classified as C-DBPs (TCM, DCP and TCP) and N-DBPs (TCAN, DCAN and TCNM). Figure 4 presents relationships between concentrations of DBPs and pre-oxidation agent doses. As observed from the results, the major DBPs were TCM and DCAN. Without pre-oxidation, the concentration of TCM was about 180 μg L^{-1}, and TCM and DCP yields continuously reduced with increasing PM doses. However, for the PM pre-oxidation, there is no obvious difference under different initial PM concentration after one-way analysis of variance (ANOVA). While for the PM/BS process, there is a significant increase ($p < 0.01$) with the increase in initial PM to BS concentrations. Figure 4b,d displays the DBPs formation potentials of NOM after pre-oxidation by PM/BS. Generally, the yields of C-DBPs exhibited the same variations, and the removal of TCM peaked at 18.2% when PM/BS was 50:250 μM. However, pre-oxidation with PM/BS continuously increased DCAN formation with increasing PM/BS doses, which was different to the trend of DCAN formation during the PM pre-oxidation process. This is probably because the system of PM/BS oxidized some functional groups and that somehow facilitated DCAN formation.

3.2.2. Effects of Pre-Oxidation Time

The pre-oxidation time was an important factor for the formation of DBPs. In this study, pre-oxidation experiments were conducted for the period of 0 to 60 min (0, 1, 10, 30 and 60 min) in the presence of HA (3 mg L^{-1}), PM (50 μM) and BS (250 μM). Results regarding the concentration of DBPs are shown in Figure 5. The TCM formation declined in the initial stage and then increased with prolonged pre-oxidation time. It was observed

that the yields of TCM exhibited the lowest upon the pre-oxidation of PM to BS at 1 min. It can be ascribed to the abundant active species that generated during the process of PM/BS pre-oxidation which occurred in a short time, and thus the precursors of DBPs were partly removed, as shown in Figure 5a. Enhanced formation of 1,1-DCP and 1,1,1-TCP were observed by increasing the pre-oxidation time. This change can be explained by the stability of DBPs. With the reaction carried on, 1,1-DCP accumulated gradually while 1,1,1-TCP hydrolyzed into TCM due to its weak stability. Interestingly, as depicted in Figure 5b, in the presence of BS, the formation of 1,1,1-TCP was rather different from that observed in the PM pre-oxidation process. With regard to the N-DBPs, the formation potential of DCAN increased remarkably, while the pre-oxidation time had no evident effect on the yields of TCAN and DCAN. As reported previously, DCAN was the main N-DBP during chlorination of water that contained NOM. The abovementioned phenomenon was different from a previous study that explored the effects of pre-oxidation time of potassium ferrate on the formation of chlorination DBPs [18]. With pre-oxidation time increased, the concentration of TCM decreased. Moreover, TCNM had an initial increase, and then reduced with reaction time.

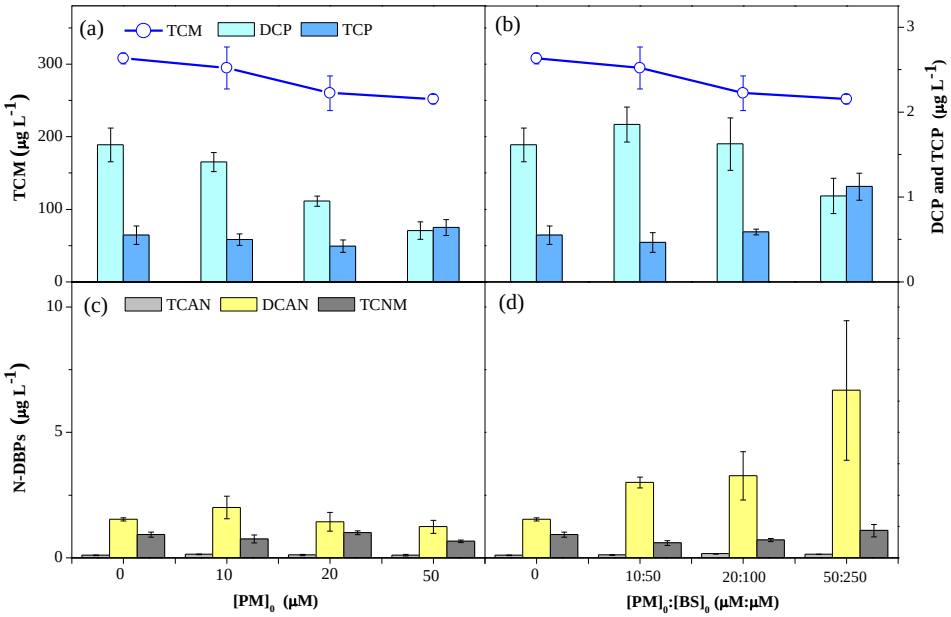

Figure 4. Effect of PM (**a**,**c**) and PM/BS (**b**,**d**) doses on the formation potential of C-DBPs and N-DBPs. ($(HA)_o$ = 3 mg L^{-1}, $(PM)_o$ = 0–50 μM, $(BS)_o$ = 0–250 μM and t = 30 min). Duplicated samples were analyzed.

3.2.3. Effect of pH

As depicted in Figure 6, pH is a vital factor influencing the existence of NOM and the formation potential of DBPs. For both the PM and PM/BS systems, the concentration of TCM increased remarkably with pH increased from 5.5 to 8.5, which is in accordance with previous studies. The TCM concentration enhanced 149.7 μg L^{-1} to pH 8.5 compared to pH 5.5. The pH of the aqueous solution can affect the hydrolysis rate of unstable by-products. The concentration of TCM generated from other unstable disinfection by-products increased under alkaline conditions. The formation potential of 1,1-DCP and 1,1,1-TCP exhibited a declining trend under PM pre-oxidation with pH increased from 5.5 to 8.5, whereas the total amount was higher than HA alone. The reaction kinetics and oxidation pathway of PM were greatly influenced by pH. In general, acidic circumstances favored the oxidation ability of PM. However, under alkaline circumstances, the organic matter cannot be completely oxidized by PM, but it will promote the destabilization of colloid and facilitate the removal of organic matter during the coagulation process. It is noted that the formation potential of DBPs reached a plateau at pH 6.5.

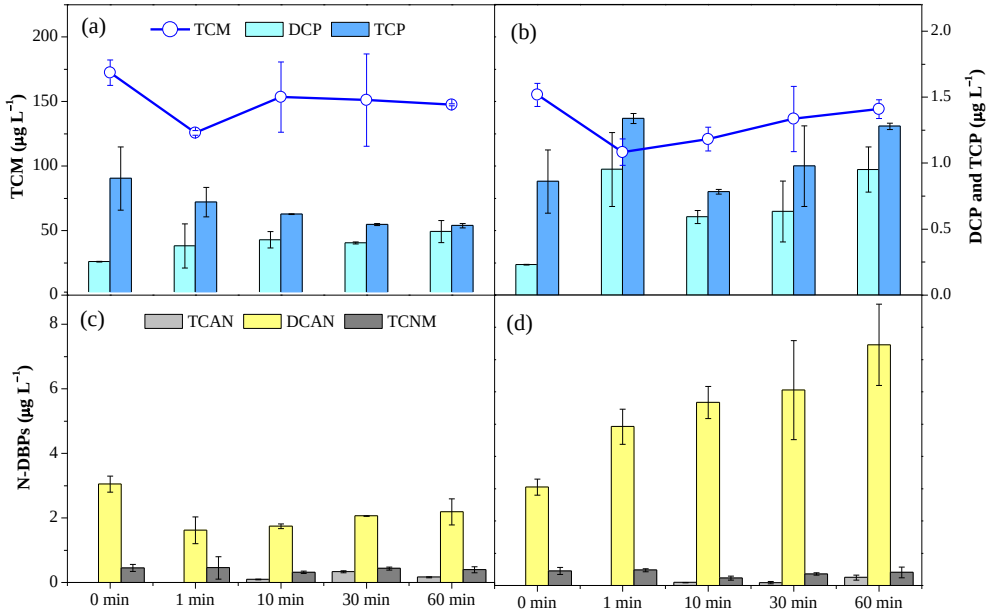

Figure 5. Effect of pre-oxidation time on the formation potential of C-DBPs and N-DBPs: (**a**,**c**) for PM process and (**b**,**d**) for PM/BS process. ($(HA)_o$ = 3 mg L^{-1}, $(PM)_0$ = 50 μM, $(BS)_o$ = 250 μM and t = 0–60 min). Duplicated samples were analyzed.

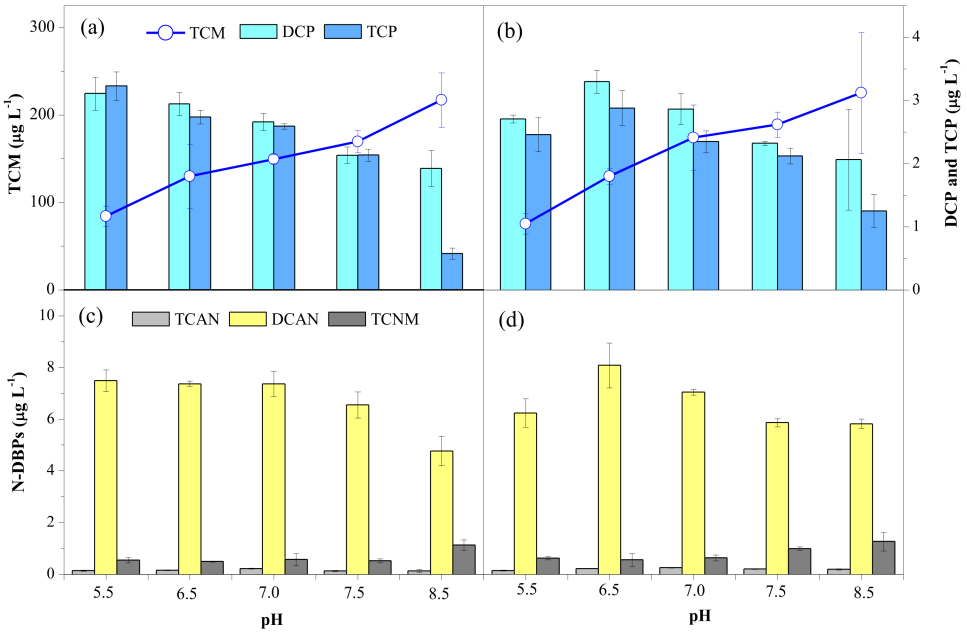

Figure 6. Effect of pH on the formation potential of C-DBPs and N-DBPs: (**a**,**c**) for PM process; (**b**,**d**) for PM/BS process. ($(HA)_o$ = 3 mg L^{-1}, $(PM)_o$ = 50 μM, $(BS)_o$ = 250 μM and pH = 5.5–8.5). Duplicated samples were analyzed.

3.2.4. Effect of Br^-

The presence of bromide ion (Br^-) influences the formation of disinfection by-products gradually. To further illustrate the role of Br^-, Br^- was introduced at various concentrations, i.e., 0.1, 0.5, 1.0 and 2.0 mg L^{-1}. The effects of Br^- on the formation potential of DBPs are demonstrated in Figure 7. The main Br-DBPs detected in this experiment were bromochloroacetonitrile (BCAN), tribromomethane (TBM) and dibromochloromethane (DBCM). In the PM system, the concentration of TCM decreased gradually with Br^- increasing from 0.1 to 2 mg L^{-1}. It can be proposed that Br^- may compete with NOM to form Br-

DBPs with chlorine. The formation potential of DBCM and BCAN also decreased with the concentration of Br^- increasing, whereas the yields of TCNM and 1,1,1-TCP increased obviously. The introduction of Br^- facilitated the formation of TCNM compared to previous experiments. These results were inconsistent with the findings that investigated the effect of Br^- on the conversion of DBPs in chlorine and chloramines. It can be found that Br^- promoted the formation of DCAN and TCP [14]. As shown in Figure 7b, the total amount of DBPs decreased remarkably with PM/BS pre-oxidation. When Br^- was 2 mg L^{-1}, the total formation potential of DBPs decreased to 150 μg L^{-1}. Additionally, other DBPs showed a similar trend with the PM system.

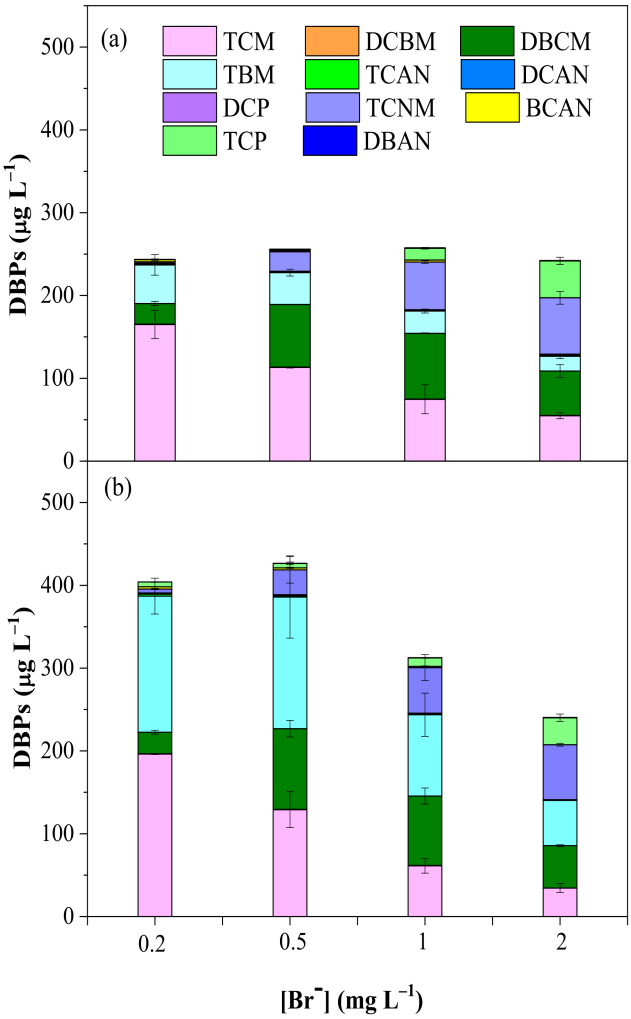

Figure 7. Effect of Br^- on the formation potential of DBPs: (**a**) PM process and (**b**) PM/BS process. ($(HA)_o$ = 3 mg L^{-1}, $(PM)_o$ = 50 μM, $(BS)_o$ = 250 μM and $(Br^-)_o$ = 0.1–2 mg L^{-1}). Duplicated samples were analyzed.

3.3. Calculated Toxicity Analysis

In order to provide a comprehensive toxicity assessment based on investigating DBPs, a cytotoxicity index (CTI) was calculated by multiplying the molar concentration (CX) of each DBP by its cytotoxicity value (1/%C1/2X) from previous studies and then summing values for all selected DBPs (TCM, DCAN, TCAN and TCNM). The calculations via Equation (1) are shown below [19–21].

$$CTI = \sum[\frac{1}{\%C1/2X} \times CX] \quad (1)$$

CTI : cytotoxicity index of the selected DBPs;

1. CX: molar concentration of each DBP;
2. %C1/2X: concentration of each DBP that induced a cell density of 50%.

As shown in Figure 8, higher PM doses decreased the CTI. However, a general increase in CTI was observed with PM/BS pre-oxidation. These demonstrated that PM/BS pre-oxidation had a negative effect on risk control of overall cytotoxicity.

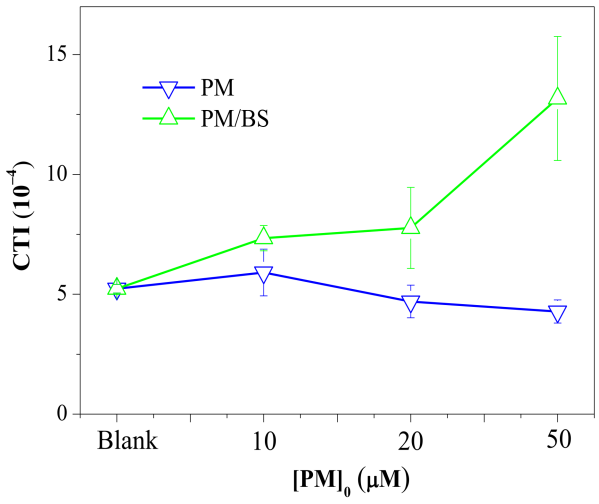

Figure 8. Changes of CTI in different doses of PM and BS. ($(HA)_o$ = 3 mg L^{-1}, $(PM)_o$ = 0–50 μM, $(BS)_o$ = 0–250 μM and t = 30 min). Duplicated samples were analyzed.

4. Conclusions

UV-Vis, TOC and 3D-EEM were applied to investigate the characteristics of NOM. Effects of PM and BS doses, pre-oxidation time, pH of solutions and concentration of Br^- on the formation potential of DBPs were examined in this study. The following conclusions can be drawn based on the experimental results:

1. TOC removal reached a plateau when the molar ratio of PM to BS was 1:5.
2. Increasing ratios of PM to BS decreased the intensity and area of fluorescence spectroscopy.
3. PM and BS doses, pre-oxidation time, pH of solutions and concentration of Br^- impacted the formation potential of various DBPs.
4. PM/BS pre-oxidation decreased the formation of TCM while increasing the yields of N-DBPs, thus increasing the risk of water quality.

Supplementary Materials: The following supporting information can be downloaded at: https://www.mdpi.com/article/10.3390/w14030507/s1, Figure S1: TOC removal obtained from different doses of PM and BS. Figure S2: The fluorescence excitation-emission matrices in different systems. Figure S3: The fluorescence excitation–emission matrices in different molar ratio of PM and BS.

Author Contributions: Conceptualization, methodology, investigation, writing—original draft preparation, S.H.; review and editing, N.R. All authors have read and agreed to the published version of the manuscript.

Funding: This research was funded by Shenzhen Science and Technology Program, grant number KQTD20190929172630447.

Institutional Review Board Statement: Not applicable.

Informed Consent Statement: Not applicable.

Acknowledgments: This work was financially supported by Shenzhen Science and Technology Program (Grant No. KQTD20190929172630447).

Conflicts of Interest: The authors declare no conflict of interest.

References

1. Ohanian, E.V.; Mullin, C.S.; Orme, J. Health effects of disinfectants and disinfection by-products: A regulatory perspective. *Water Chlorination Environ. Impact Health Eff.* **1990**, *2*, 75–86.
2. Richardson, S.D.; Plewa, M.J.; Wagner, E.D.; Schoeny, R.; De Marini, D. Occurrence, genotoxicity, and carcinogenicity of regulated and emerging disinfection by-products in drinking water: A review and roadmap for research. *Mutat. Res. Mutat. Res.* **2007**, *636*, 178–242. [CrossRef] [PubMed]
3. Costet, N.; Villanueva, C.M.; Jaakkola, J.J.K.; Kogevinas, M.; Cantor, K.P.; King, W.D.; Lynch, C.F.; Nieuwenhuijsen, M.J.; Cordier, S. Water disinfection by-products and bladder cancer: Is there a European specificity? A pooled and meta-analysis of European case-control studies. *Occup. Environ. Med.* **2011**, *68*, 379–385. [CrossRef] [PubMed]
4. Hua, G.; Reckhow, D.A. Characterization of Disinfection Byproduct Precursors Based on Hydrophobicity and Molecular Size. *Environ. Sci. Technol.* **2007**, *41*, 3309–3315. [CrossRef] [PubMed]
5. Li, X.-F.; Mitch, W.A. Drinking Water Disinfection Byproducts (DBPs) and Human Health Effects: Multidisciplinary Challenges and Opportunities. *Environ. Sci. Technol.* **2018**, *52*, 1681–1689. [CrossRef] [PubMed]
6. Roccaro, P.; Vagliasindi, F.G.A. Differential vs. absolute UV absorbance approaches in studying NOM reactivity in DBPs formation: Comparison and applicability. *Water Res.* **2009**, *43*, 744–750. [CrossRef] [PubMed]
7. Roccaro, P.; Chang, H.-S.; Vagliasindi, F.G.; Korshin, G.V. Differential absorbance study of effects of temperature on chlorine consumption and formation of disinfection by-products in chlorinated water. *Water Res.* **2008**, *42*, 1879–1888. [CrossRef] [PubMed]
8. Sanly, L.M.; Chiang, K.; Amal, R.; Fabris, R.; Chow, C.; Drikas, M. A Study on the Removal of Humic Acid Using Advanced Oxidation Processes. *Sep. Sci. Technol.* **2007**, *42*, 1391–1404. [CrossRef]
9. Von Gunten, U. Disinfection and byproduct formation in presence of bromide, iodide or chlorine. *Water Res.* **2003**, *37*, 1469–1487. [CrossRef]
10. Mao, Y.; Wang, X.; Yang, H.; Wang, H.; Xie, Y.F. Effects of ozonation on disinfection byproduct formation and speciation during subsequent chlorination. *Chemosphere* **2014**, *117*, 515–520. [CrossRef] [PubMed]
11. Li, C.; Li, X.; Graham, N. A study of the preparation and reactivity of potassium ferrate. *Chemosphere* **2005**, *61*, 537–543. [CrossRef] [PubMed]
12. Xu, L.; Dong, H.; Xu, K.; Li, J.; Qiang, Z. Accelerated degradation of pesticide by permanganate oxidation: A comparison of organic and inorganic activations. *Chem. Eng. J.* **2019**, *369*, 1119–1128. [CrossRef]
13. Duan, S.; Hou, P.; Yuan, X.; Stanic, M.; Qiang, Z.; Dong, H. Homogeneous activation of bisulfite by transition metals for micro-pollutant degradation: Mn (VII) versus Cr (VI). *Chem. Eng. J.* **2020**, *394*, 124814. [CrossRef]
14. Liu, C.; Zhao, M.; He, S.; Cao, Z.; Chen, W. Activation of permanganate with hydrogen sulfite for enhanced oxidation of a typical amino acid. *Environ. Technol.* **2018**, *40*, 1605–1614. [CrossRef] [PubMed]
15. Gao, Y.; Jiang, J.; Zhou, Y.; Pang, S.-Y.; Ma, J.; Jiang, C.; Wang, Z.; Wang, P.-X.; Wang, L.-H.; Li, J. Unrecognized role of bisulfite as Mn(III) stabilizing agent in activating permanganate (Mn(VII)) for enhanced degradation of organic contaminants. *Chem. Eng. J.* **2017**, *327*, 418–422. [CrossRef]
16. USEPA. *Method 551.1. Determination of Chlorination Disinfection by Products, Chlorinated Solvents, and Halogenated Pesticides/Herbicides in Drinking Water by Liquid-Liquid Extraction and Gas Chromatography with Electron-Capture Detection*; National Exposure Research Laboratory Office of Research and Development: Cincinnati, OH, USA, 1995.
17. Huang, S.; Gan, W.; Yan, M.; Zhang, X.; Zhong, Y.; Yang, X. Differential UV–vis absorbance can characterize the reaction of organic matter with ClO_2. *Water Res.* **2018**, *139*, 442–449. [CrossRef] [PubMed]
18. Gan, W.; Sharma, V.; Zhang, X.; Yang, L.; Yang, X. Investigation of disinfection byproducts formation in ferrate(VI) pre-oxidation of NOM and its model compounds followed by chlorination. *J. Hazard. Mater.* **2015**, *292*, 197–204. [CrossRef] [PubMed]
19. Krasner, S.W.; Weinberg, H.S.; Richardson, S.D.; Pastor, S.J.; Chinn, R.; Sclimenti, M.J.; Onstad, G.D.; Thruston, A.D. Occurrence of a New Generation of Disinfection Byproducts. *Environ. Sci. Technol.* **2006**, *40*, 7175–7185. [CrossRef] [PubMed]
20. Plewa, M.J.; Wagner, E.D.; Muellner, M.G.; Hsu, K.-M.; Richardson, S.D. *Comparative Mammalian Cell Toxicity of N-DBPs and C-DBPs*; ACS Symposium Series; Oxford University Press: Oxford, UK, 2007; Volume 3, pp. 36–50.
21. Plewa, M.J.; Wagner, E.D. Charting a new path to resolve the adverse health effects of DBPs, Chapter 1. In *Recent Advances in Disinfection By-Products*; Karanfil, T., Mitch, B., Westerhoff, P., Xie, Y., Eds.; American Chemical Society: Washington, DC, USA, 2015; pp. 3–23.